Available online at www.sciencedirect.com

ScienceDirect

Procedia Engineering 193 (2017) 455 – 461

Procedia Engineering

www.elsevier.com/locate/procedia

International Conference on Analytical Models and New Concepts in Concrete and Masonry Structures AMCM'2017

Modelling of deformable polymer to be used for joints between infill masonry walls and R.C. frames

Matija Gams[a]*, A. Kwiecień[b], J. Korelc[c], T. Rousakis[d] and A. Viskovic[e]

[a]*ZAG - Slovenian National Building and Civil engineering Institute, Dimičeva 12, 1000 Ljubljana, Slovenia*
[b]*Cracow University of Technology, Institute of Structural Mechanics, Warszawska 24, 31-155 Kraków, Poland*
[c]*University of Ljubljana, Faculty for Civil and Geodetic Engineering, Jamova 2, 1000 Ljubljana, Slovenia*
[d]*Democritus University of Thrace, Department of Civil Engineering,Vas Sofias 12, 67100 Xanthi, Greece*
[e]*D'Annunzio University of Chieti-Pescara, Engineering and Geology Department,Viale Pindaro 42, 65127 Pescara, Italy*

Abstract

In the paper an idea to use a deformable polymer material for the joint between R.C. frames and masonry infills is presented. As an early step of testing the idea, experimental tests of the polymer in monotonic uniaxial tension at different load rates are performed and analyzed. The load rates range from very fast (8.3 mm/s) to very slow (0.00083 mm/s). The material exhibits a very strong strain rate effect and viscous behavior. In the second part of the paper a numerical model is developed and implemented into a finite element to simulate the results of the tests. The model is based on a new family of strain measures, called the Darjani-Naghdabadi strain measures and a classical viscosity formulation. Almost perfect model predictions up to collapse at 50-150 % elongation are obtained by using calibration based on minimization of error.

Peer-review under responsibility of the scientific committee of the International Conference on Analytical Models and New Concepts in Concrete and Masonry Structures

Keywords: masonry infills; deformable polymer joint; viscosity; modelling;

* Corresponding author. Tel.: +386 31 377 246
E-mail address: matija.gams@zag.si

Peer-review under responsibility of the scientific committee of the International Conference on Analytical Models and New Concepts in Concrete and Masonry Structures
doi:10.1016/j.proeng.2017.06.237

1. Introduction

Masonry infills are commonly used in old residential buildings and office buildings, as well as in new buildings around the world. The infills can be built from different types of masonry, some of which could even be used for load-bearing walls, but the infills are generally not considered as load bearing elements, or are even prohibited by codes to be used as such [1]. Nevertheless, the infills contribute to lateral stiffness as well as to resistance of the composite frame-infill system and are rigidly connected to the frame. Due to length of the infills walls, they are often stiffer than the surrounding frame and therefore attract forces quickly. This in combination with the brittle nature of masonry [2] means that serious damage to infills can occur at relatively modest earthquake intensity, when the frame has not yet developed significant damage (Figure 1).

Fig. 1. Collapse of infills in a negligibly damaged rc frame (Pescala del Tronto, Italy, 2016).

In an attempt to alleviate this problem, an idea to separate the infill wall and the R.C. frame by a deformable but strong enough material was born. A material perfectly suitable for this purpose, called polymer PM, was found. The material is special polyurethane with patented additives, and has the following properties: Young's modulus E = 4.5 MPa, tensile strength f_t = 0.85÷1.95 MPa, ultimate strain ε_u = 50÷150% (depending on the strain rate of load application). This material was tested in many practical applications between structural elements [3, 4, 5], including dynamic [6], shear [7, 8] and bending tests [8, 9]. The flexibility of the polymer could serve to reduce the stress concentrations and thereby reduce damage to infills on one hand, and provide a high amount of damping and ductility on the other. Despite the flexibility of the polymer, the brick-to-concrete joint would be capable of transferring significant loads during in-plane and out-of-plane excitations. Polymer PM flexible joints manifested this ability in laboratory shear tests, carried out between concrete (Fig. 2) and clay brick (Fig. 3) substrates. The flexible joints made of polymer PM [10] were able to transfer shear strain up to 100% and shear stress over 0.8 MPa (Fig 3).

To test the idea, the polymer first had to be tested experimentally and numerically modelled in simple load scenarios such as pure tension and pure shear. The first attempts at modelling [10, 11] have shown, that the material is difficult to model under high strains, as the standard hyperelastic models based on Seth-Hill [12] strain measures are not accurate enough. In order to improve the accuracy of the numerical simulation special strain measures have to be used. The special strain measures are of the Darjani-Naghdabadi (D-N) type [13] which has two parameters for calibration instead of only one of the Seth-Hill family of strain measures.

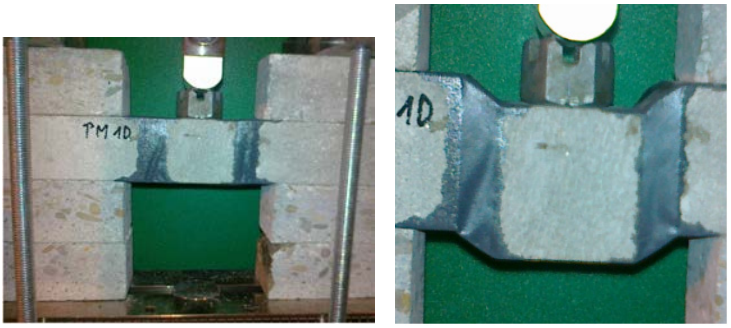

Fig. 2. Deformation of polymer flexible joint made of polymer PM between concrete substrates – after [11].

a)

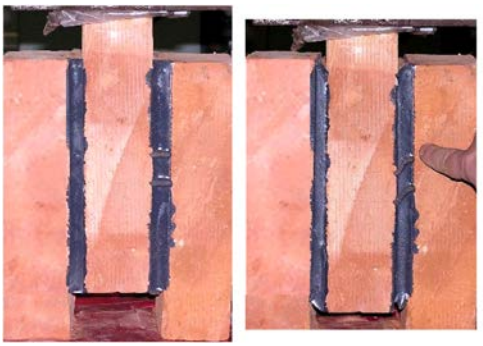

b)

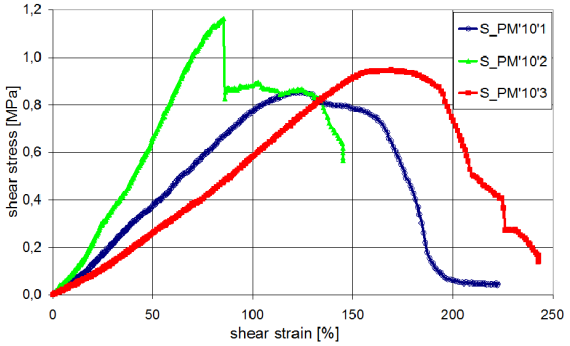

Fig. 3. Deformation of polymer flexible joint made of polymer PM between clay brick substrates (a) and the shear stress-strain characteristic of polymer flexible joint made of polymer PM. (b) – after [11].

In this paper, the simple monotonic tensile tests performed at different rates are presented and the response is numerically simulated. In order to be able to numerically model the viscosity, the hyperelastic model is upgraded with a basic viscosity formulation. Numerical results show high versatility and accuracy of the model in modelling monotonic uniaxial tensile response at different load rates and show an almost perfect match with the experiments.

Nomenclature

E	Young's modulus
f_t	tensile strength
ε_u	ultimate strain
$\mathbf{E}^{(m)}$	Seth-Hill strain measures
$\mathbf{U}$	right stretch tensor
$\mathbf{E}^{(\alpha,\beta)}$	Darjani-Naghdabadi strain measures
m	parameter of the Seth-Hill strain measures (real number)
α,β	parameters of the Darjani-Naghdabadi strain measures (real numbers)
λ_i	principal stretch in i-th direction
Λ,μ	Lame constants
κ, ν	Bulk modulus, Poisson ratio
$\mathbf{I}$	Identity matrix
t_r	relaxation time
q	auxiliary variable

2. Experimental testing

Pure tensile tests were performed on dogbone specimens (Fig. 4a) according to ISO 527 standard [14], using universal testing machine Zwick 1455 with the long distance extensometer. The cross section of the dogbone specimen was 10 mm x 4 mm. The length of the specimen between the extensometer sensors was 50 mm and displacement control with the extensometer was applied. Five different strain ratio of the test was used: 10^{1}/min, 10^{0}/min, 10^{-1}/min, 10^{-2}/min and 10^{-3}/min, where 6 specimens in each series were tested (except the strain ratio 10^{-3}/min test with 1 specimen tested). Failure modes of specimens are presented in Fig. 4b.

Results of tests are shown in Figs. 4 – 6. It is clear from the results, that the effect of the load rate on response is very high. The tensile strength and ultimate strain at fracture are about 2 MPa and 150 %, respectively, for the highest strain rate (10^{1}/min) – similar to dynamic action during earthquake. In case of the smallest strain rate (10^{-3}/min) – similar to quasi-static action during changes of thermal loads, the tensile strength and ultimate strain at fracture are about 1.1 MPa and 90 %, respectively.

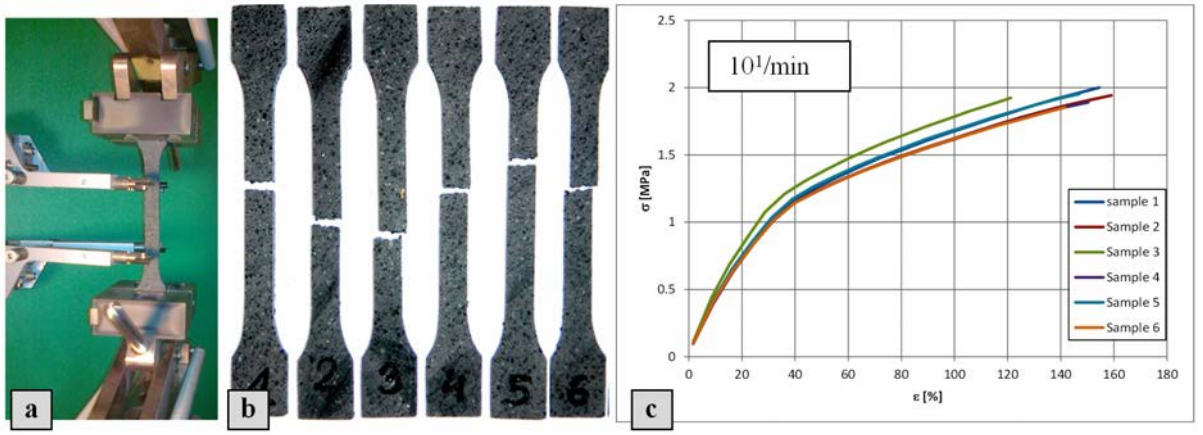

Fig. 4. Polymer PM in the universal testing machine with long distance extensometer (a), failure modes of dogbone polymer PM specimens (b), stress-strain response of samples loaded with strain rate 10^{1}/min (c).

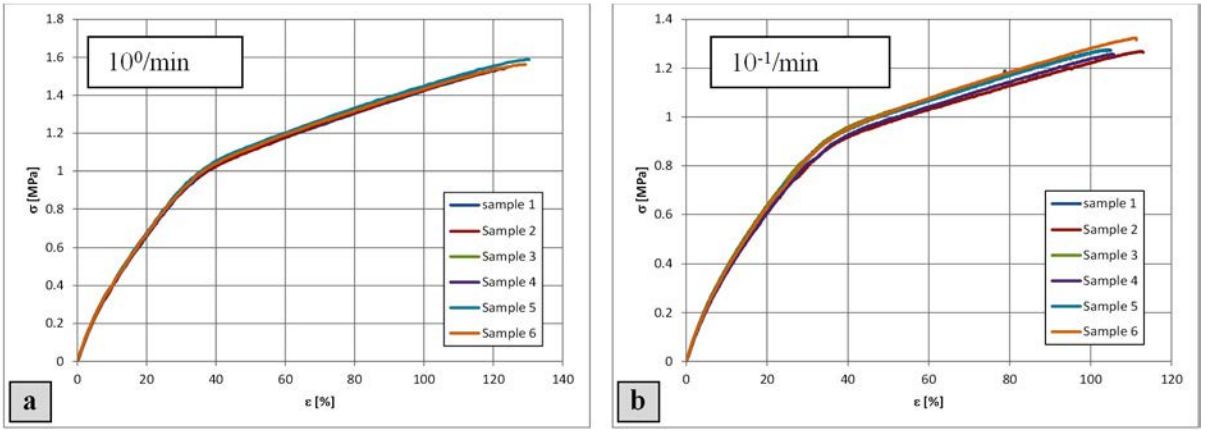

Fig. 5. Stress-strain response of samples loaded with strain rate 10^{0}/min (a) and 10^{-1}/min (b).

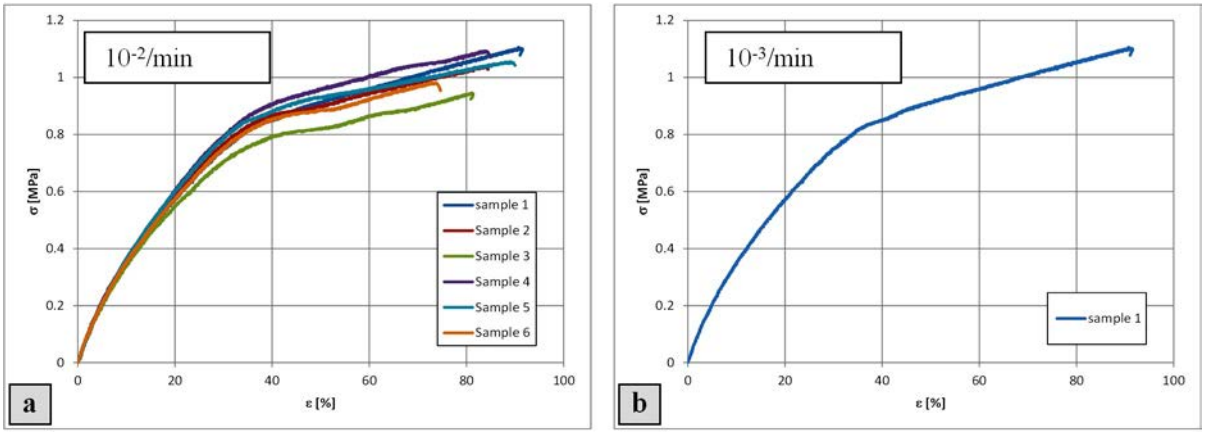

Fig. 6. Stress-strain response of samples loaded with strain rate 10^{-2}/min (a) and 10^{-3}/min (b).

3. Constitutive modelling

As shown by experimental testing in the previous section, the viscous effect of the material is very pronounced and has to be taken into account in order to properly model the dynamic response. Furthermore, the material exhibits strongly nonlinear behavior, which cannot be accurately modelled using Saint-Venant-Kirchhoff (SVK) material and Seth-Hill strain measures $\mathbf{E}^{(m)}$ [11, 12, 13]. It has been shown in e.g. [10, 11, 15], that the best solution using a SVK material based on $\mathbf{E}^{(m)}$ strains is obtained for the special case m = 0, which is also called Hencky or logarithmic strains, but even this model is not accurate enough [11, 13, 16, 17, 18]. In order to improve the accuracy of the SVK material a new family of strain measures [16] and its modification, called the Darjani-Naghdabadi (D-N) strains [13] has to be used. These strain measures have two parameters (α and β), whereas the Seth-Hill family of strains only has one parameter (m). The objective D-N strains $\mathbf{E}^{(\alpha,\beta)}$ are defined by Eq. (1), where $\mathbf{U}$ is the right stretch tensor.

$$\mathbf{E}^{(\alpha,\beta)} = \frac{1}{\alpha+\beta}\left(\mathbf{U}^{\alpha} - \mathbf{U}^{-\beta}\right) \tag{1}$$

The conjugate stresses $\mathbf{T}^{(\alpha,\beta)}$ are also objective and can be defined by Eq. (2), using principal principle stretches λ_i.

$$\mathbf{T}^{(\alpha,\beta)} = \frac{2\mu}{\alpha+\beta}\begin{bmatrix} \lambda_1^{\alpha}-\lambda_1^{-\beta} & & \\ & \lambda_2^{\alpha}-\lambda_2^{-\beta} & \\ & & \lambda_3^{\alpha}-\lambda_3^{-\beta} \end{bmatrix} + \frac{\Lambda}{(\alpha+\beta)}\left(\lambda_1^{\alpha}-\lambda_1^{-\beta}+\lambda_2^{\alpha}-\lambda_2^{-\beta}+\lambda_3^{\alpha}-\lambda_3^{-\beta}\right)\begin{bmatrix} 1 & & \\ & 1 & \\ & & 1 \end{bmatrix} \tag{2}$$

In case of $m = \alpha + \beta = 0$ the D-N strains also simplify to the Hencky (logarithmic) strains. The form of strain energy remains the same as the SVK model and is shown in Eq. (3) with the Lame constants μ and Λ.

$$W\left(\mathbf{E}^{(\alpha,\beta)}\right) = \mu\, tr\left(\mathbf{E}^{(\alpha,\beta)}\right)^2 + \frac{\Lambda}{2}\left(tr\,\mathbf{E}^{(\alpha,\beta)}\right)^2 \tag{3}$$

The model presented in Eqs. (1) – (3) was augmented by the classical viscosity model [19], which is based on the split to volumetric ($\mathbf{T}_v$) and deviatoric ($\mathbf{T}_d$) stresses and the change of the shape related to deviatoric component to account for time effects.

$$T_v = \kappa\, tr\left(\mathbf{E}^{(\alpha,\beta)}\right)\mathbf{I} \tag{4}$$

$$T_d = 2\mu\left((1-\nu)E_d + \nu q\right) \tag{5}$$

In Eqs. (4) and (5) κ is the bulk modulus, **I** is the identity matrix and ν is the Poisson ratio. q is an auxiliary variable, defined as:

$$\boldsymbol{q} = \frac{t_r}{t_r+\Delta t}\mathbf{E}_d + \frac{t_r}{(t_r+\Delta t)}(\boldsymbol{q}_n - \mathbf{E}_{d,n}) \tag{6}$$

Here, subscript *n* denotes previous time step, Δ*t* is time step and t_r is the so-called relaxation time. $\mathbf{E}_d$ and $\mathbf{E}_{d,n}$ are the deviatoric part of the D-N strains, and the deviatoric part of the D-N strains in the previous time step, respectively.
The material model described in Eqs. (1)-(6) was implemented into a 3D finite element using AceGen [20], a system for automatic generation of a finite-element code [21, 22].

4. Numerical simulations

Using the above presented hyperviscoelastic formulation, a very good correlation with experimental tests can be obtained. The match was found using numerical minimization of response curves in two phases. In the first phase, the relaxation time was sought and was determined to be t_r =25000 s. In the second phase such values of α and β were sought that gave the best correlation with the experiment. Again, numerical minimization using routines built into Mathematica were used. Different values of parameters α and β had to be used for different load rates to get a good correlation. In the calculations Poisson's ratio was assumed to be ν = 0.49. The results are summarized in Table 1 and in Figure 7.

Table 1. Parameters of the model for different strain rates.

N	1	2	3	4	5
Strain rate [1/min]	10^1	10^0	10^{-1}	10^{-2}	10^{-3}
α [-]	0.8	0.87	0.85	0.97	1.0
β [-]	1.15	1.53	1.64	1.96	1.43
t_r [s]	25000	25000	25000	25000	25000

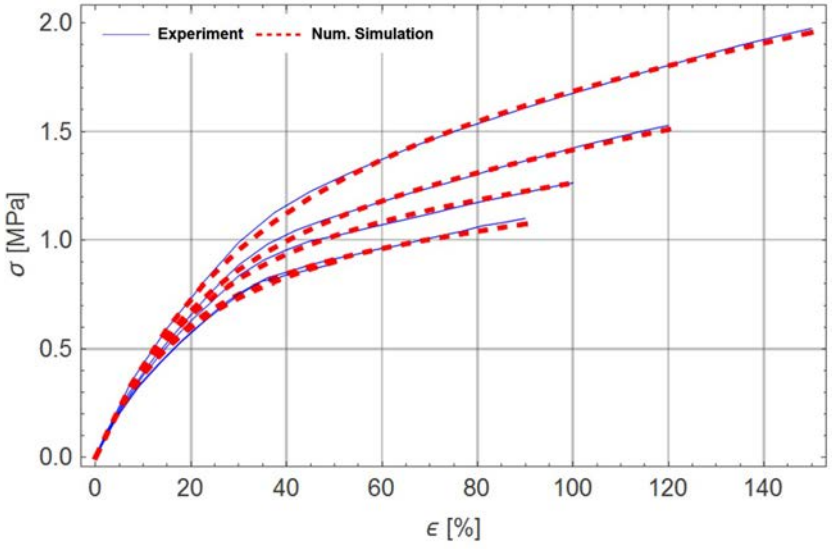

Fig. 7. Experimental stress-strain response vs. numerical simulation

5. Conclusions

The idea of using flexible, yet strong polymer joints between the R.C. frame and the masonry is presented in the paper. One of the first steps of developing the idea is to use or develop proper material models for simulation of seismic response. In the first stage a series of experiments in monotonic uniaxial tension was performed at different strain rates (25 tests). Because existing models for rubberlike materials based on Seth-Hill family of strains cannot simulate the response accurately enough, a new model based on different strain measures had to be used. A new constitutive model based on the so called Darjani-Naghdabadi strain measures and classical viscosity was developed and implemented into finite element code. Using the newly developed constitutive model and finite element, the response of the experiments was numerically modelled. A special algorithm for finding the best parameters of the constitutive model based on numerical minimization was used and the results give an almost perfect match between the tests and the calculations. In future, the model will be upgraded to include also cyclic behaviour and will be implemented into numerical models for seismic response of R.C. frames with infills, separated by the flexible polymer joints.

References

[1] CEN EN 1998-1.Eurocode 8: Design of structures for earthquake resistance - Part 1: General rules, seismic actions and rules for buildings .
[2] M. Tomaževič, Eartquake-resistant design of masonry buildings, Imperial College Press, London, 1999.
[3] A. Kwiecień, Highly deformable polymers for repair and strengthening of cracked masonry structures, GSTF International Journal of Engineering Technology (JET) Vol.2 No.1 (May 2013) 182-196.
[4] A. Kwiecień, M. Gruszczyński, B. Zając, Tests of flexible polymer joints repairing of concrete pavements and of polymer modified concretes influenced by high deformations, Trans Tech Publications 2011. Key Engineering Materials Vol. 466 (2011), pp. 225-239.
[5] A. Kwiecień, P. Kuboń, B. Zając, Numerical analysis of cracked masonry building excited by an earthquake after repair using polymer flexible joint, Monografia nr 482 Recent advances in civil engineering: structural mechanics (Ed. K. Stypuła), Wydawnictwo Politechniki Krakowskiej, Seria Inżynieria Lądowa, Kraków (2015), pp. 63-79.
[6] R. Jankowski, A. Kwiecień, Experimental study on polymer mass used to repair damaged structures, Key Engineering Materials 488-489: (2012) 347-50.
[7] Kisiel P., The stiffness and bearing capacity of Polymer Flexible Joint under shear load. Procedia Engineering 108 (2015): 496 – 503.
[8] P. Kisiel, H. Ciurej, A. Kwiecień, Experimental and numerical study of connection subjected to bending in airfield pavement, Logistyka nr 4/2014, pp. 4414-4424.
[9] P. Kisiel, Z. Mikulski, A. Kwiecień, J. Adamus, The use of Polymer Flexible Joint technology in tramway tracks construction, Logistyka nr 4/2014, pp. 4437-4444.
[10] A. Kwiecień, Polymer flexible joints in masonry and concrete structures (in Polish), Monography No. 414, Wyd. Politechniki Krakowskiej, Seria Inżynieria Lądowa, Kraków, 2012.
[11] A. Kwiecień, M. Gams, B. Zając, Numerical modelling of flexible polymers as the adhesive for FRPs. FRPRCS-12 & APFIS-2015 Joint Conference, Nanjing, China, 2015.
[12] B. R. Seth, Generalized strain measure with applications to physical problems. Second-Order Effects in Elasticity, Plasticity, and Fluid Dynamics, Pergamon Press, Oxford 1964.
[13] H. Darijani, R. Naghdabadi, Constitutive modeling of solids at finite deformation using a second-order stress-strain relation, International Journal of Engineering Science, 48(2010) 223-236.
[14] EN ISO 527-1, Plastics-determination of tensile properties – Part 1: general principles; 2012.
[15] A. Kwiecień, Modeling of constitutive equations for hyperelastic polymers in flexible joints, Modern Structural Mechanics in Engineering Design Studies in the Field of Engineering, No. 92, PAN KILiW, [in Polish], Politechnika Warszawska, Warszawa, 2015, pp. 153–180.
[16] Z.P. Baˇzant, Easy-to-compute tensors with symmetric inverse approximating Hencky finite strain and its rate, Journal of Engineering Materials and Technology, Transactions of the ASME, 120(2) , 1998, pp. 131–136.
[17] S. Jemioło, Study of hyperelastic properties of isotropic materials. Modeling and numerical implementation, Scientific Works. Civil Engineering., Nr 140, OWPW, Warszawa 2002.
[18] S. Jemioło, Constitutive relationships of hyperelasticity. PAN, KILiW. Warszawa 2016.
[19] P. Wriggers, Nonlinear Finite Element Methods, Springer Berlin Heidelberg, 2008.
[20] J. Korelc, Automatic generation of finite-element code by simultaneous optimization of expressions, Theoretical Computer Science, 187(1–2), 1997, pp. 231–248.
[21] AceGen 7.0 and AceFEM 7.0 user manual, http://symech.fgg.uni-lj.si/.
[22] B. Wcisło, J. Pamin, Entropic thermoelasticity for large deformations and its AceGen implementation, Recent Advances in Computational Mechanics, CRC Press Taylor & Francis Group, London, 2014, pp. 319–326.